

A Low-Cost Patch-Antenna for Non-Invasive Brain Cell Detection

Abdullah Alzahrani



Abstract: Cancer is one of the most and frequent causes of death around the world. Brain tumor is a critical and dangerous type and has a few difficulties of the techniques used for its detection; it is hard to determine its location when it is small at an early stage. The purpose of this work is to design a patch antenna sensor that is a low-cost microstrip which is suitable to detect a brain cancer tumor. The computer simulation technology CST Studio Suite 3D EM simulation and analysis was used to design a patch antenna with different frequencies of 2.8 GHz, 3.9 GHz, 5GHz and 5.6GHz to diagnose brain tumors. A comparison study between these resonance frequencies (lower-band (L-B) 2 GHz, middle-band (M-B) 3.9-5 GHz and upper-band (U-B) > 5 GHz) has been performed with six layers of brain phantom of fat, dura, brain, skin, CSF (Cerebrospinal Fluid) and skull. The designed patch sensor was assessed on both scenarios without and with a tumor cell on a brain phantom. Three parameters have been observed, the frequency phase shift, the deep amount of reflection return loss and power absorption were used to indicate the presence of the tumor cell. This study concludes that the middle-band (M-B) results in good penetration and better return loss depth around -20dB. Meanwhile, the higher band provides high resolution of 21 MHz phase-shift but with only depth value of difference return loss of -0.1dB. The proposed work could provide a pathway on the design of patch sensors for biomedical applications.

Keywords: Antenna; Specific Absorption Rate; Brain Tumor; Phase Shift; Return Loss.

I. INTRODUCTION

Cancer is the most threatened disease in the last 5 decades and can affect other normal body parts. Brain tumor, however, is one of the most dangerous diseases international as will influences the other tissue on human body. In the USA, 2017 around 23,800 patients of brain tumor and about 16,700 were deaths in the same year [1]. The common methods utilized to detect cancer are positron emission tomography (PET), X-ray screening, ultrasound imaging, computed tomography (CT) scan and magnetic resonance imaging (MRI) scanning [2]. Despite the variance of these techniques and their accuracy, most of them are complicated, expensive, and bulky.

One method of diagnosing brain cancer is ultrasound imaging; however, this method suffers from the quality of the images which sometimes cannot be clearly distinguished between a healthy cell and a modified cell in its initial stage [3]. In addition, this method could cause the worsening of the patients' lives due to misdiagnoses and inaccurate results in first checking [4]. The most advanced technique to examine brain cancer is magnetic resonance imaging (MRI), which is one of the sensitive techniques that can be used for dense tissues. Despite the sensitivity of MRI, it is costly and complicated. In addition, the tumor cannot be detected accurately by using this method, which may lead to mismatch the extraction or could cause other complications [5].

In previous techniques, there are still some limitations such as localization, inaccurate, bulky equipment, complicated and expensive techniques. Thus, a new method has been introduced to detect brain cancer which is based on microwave. This will allow non-invasive test, low on cost, less time and accuracy [6]. Microwave technique considered to be an active wave-based nonionizing electromagnetic and noninvasive wave which entrances human tissues without initiating health risks [7]. The main principle of using microwave technology is based on electrical properties between normal and cancerous tissues [8] [16]. Radar-constructed technique is desirable technique because it considers and focuses on the electrical properties of the tumor [9].

The antenna is the most significant element for the quality of brain tumor detection thus, appropriate antenna requirements should be considered. Such a system should cover several factors including compactness, simplicity of combination, ease geometric construct, enhanced bandwidth, tiny size, gain, and directivity [10] [17]. All the constraints can be implemented by creating a microstrip-patch antenna with light mass, low shape, planar construction, and low production cost [11] [19].

Early stages detection can be reduced treatment phase and cost [12]. Therefore, early diagnosis can save life and can reach 97% of survival [4]. However, conventional microstrip patch antenna design need adaptations for reliable wave transmission and reflected collection signal for a such brain malignant tumor detection. Thus, the goal of this research is to: (1) design confirmation of a low cost and reliable microstrip patch antenna and (2) detect a tumor-cell within the brain. In this approach, the design has numerically presented a new microstrip patch antenna designed for cancer detection in the brain. The structure design grants a consistent, and highly capable way to identify brain tumor at an initial stage. This study could be useful for biomedical applications.

Manuscript received on 24 January 2024 | Revised Manuscript received on 30 January 2024 | Manuscript Accepted on 15 February 2024 | Manuscript published on 28 February 2024.

*Correspondence Author(s)

Abdullah Alzahrani*, School of Electrical and Electronic Engineering, Taif University, Al Hawiyah, E-mail: aatyah@tu.edu.sa, ennnnng@gmail.com, ORCID ID: 0000-0002-2490-1466

© The Authors. Published by Blue Eyes Intelligence Engineering and Sciences Publication (BEIESP). This is an open access article under the CC-BY-NC-ND license <http://creativecommons.org/licenses/by-nc-nd/4.0/>.

Retrieval Number: 100.1/ijeat.C436913030224

DOI: [10.35940/ijeat.C4369.13030224](https://doi.org/10.35940/ijeat.C4369.13030224)

Journal Website: www.ijeat.org

Published By:
Blue Eyes Intelligence Engineering
and Sciences Publication (BEIESP)
© Copyright: All rights reserved.



II. METHOD

The basic principle of this work is to design microstrip patch antenna which is used to observe the reflected signals and distinguish between the different electrical properties of cells. Normal and cancerous cells can be distinguished, and they are different regarding electrical properties. Patch antenna is the most essential element that needs to be considered in the system.

The basic principle is that antenna will transmit a microwave electromagnetic into a particular part of the body, some signal scatters back to the antenna which is depending on the dielectric of the cell. According to studies [13] [15], the dielectric property of a healthy cell is lesser than a cancerous cell. Thus, it can be easily distinguished by using backscattered signal to indicate a cancerous cell presence. Furthermore, further data can be obtained from the scattered back signal that are valuable evidence such as the depth of return loss and phase shift, which reveal the existence of a cancer cell.

The direction of the radiation pattern (directivity), gain, matching feed-in, resonance frequency, efficiency and specific absorption rate SAR radiation are crucial parameters for our design to firmly detect brain cancer cells. All these parameters are considered in the antenna design. In this model, we focus on the antenna design, head phantom modeling, tumor inside the brain. The phase-shift and the SAR values human head model were considered.

A. Antenna Patch Section Formula

All the requirements of designing the patch antenna were considered such as small size, light weight, cost-effective and easy microstrip configuration. The design uses flame retardant epoxy resin and glass fabric composite (FR4) as substrate with $\epsilon_r = 4.3$, thickness $h = 1.6\text{mm}$ and loss tangent $= 0.025$. In addition, a copper ground layer is used with the

thickness $= 0.035\text{mm}$ whereas the line feed of microstrip is built as central feeding procedure to match the 50Ω . The formula of patch's dimension is given as [14] [18]:

Length of patch:

$$L = \frac{1}{2f_r \sqrt{\epsilon_{reff} \mu_0 \epsilon_0}} = -2\Delta L \tag{1}$$

Where h is substrate thickness:

$$\epsilon_{reff} = \frac{\epsilon_r + 1}{2} + \frac{\epsilon_r - 1}{2} \left[1 + 12 \frac{h}{w} \right]^{-1/2} \tag{2}$$

$$\frac{\Delta L}{h} = 0.412 \frac{(\epsilon_{reff} + 0.3) \left(\frac{w}{h} + 0.264 \right)}{(\epsilon_{reff} - 0.258) \left(\frac{w}{h} + 0.8 \right)} \tag{3}$$

Wide of patch (Wp):

$$w = \frac{1}{2f_r \sqrt{\mu_0 \epsilon_0}} \sqrt{\frac{2}{\epsilon_r + 1}} = \frac{v_0}{2f_r} \sqrt{\frac{2}{\epsilon_r + 1}} \tag{4}$$

where ϵ_r = dielectric constant of substrate

ϵ_{reff} = Effective dielectric constant

W_p = Width of the patch

B. Substrate and Ground Planes

Length of substrate plane (Ls):

$$L_s = 6h + L \tag{5}$$

Wide of substrate plane (Ws):

$$W_s = 6h + W \tag{6}$$

The ground width is identical to the substrate width.

C. Antenna Sensor Construct

The construction of patch antenna sensor and its dimensions are illustrated. At first, a simple rectangular microstrip is designed with multiple slots and different resonant frequencies. In addition, a line feeding practice is utilized to feed the antenna and 50Ω impedance is matched. The sizes and geometry of the antenna and ground structure are shown in Figure 1.

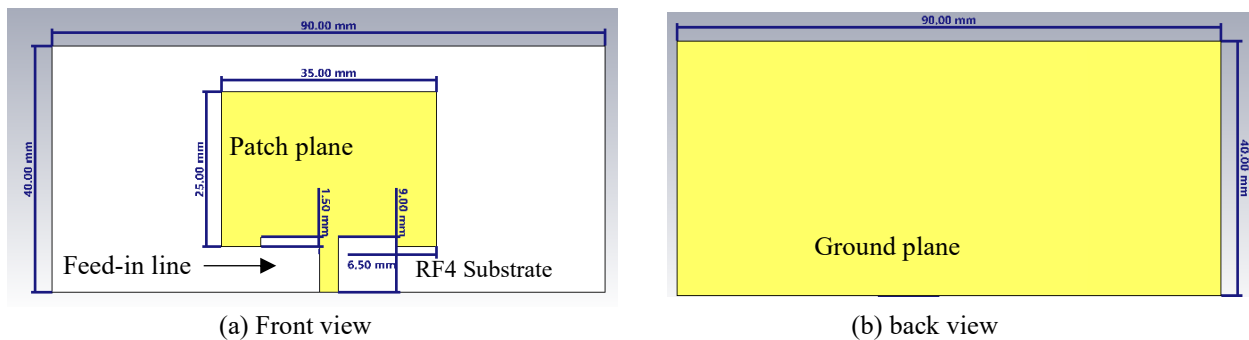


Figure 1. Structure of the Microstrip Patch Antenna, (A) Front Patch and (B) Back Patch

Figure 1 is presented with layers of microstrip patch antenna design which contains of three layers namely back ground, middle substrate, and top patch. The dimensions of antenna sensor (substrate) and patch are $40 \times 90 \text{ mm}$ and $35 \times 25 \text{ mm}$ respectively. As seen from figure 1, the back ground plane is covering the entire backside of the antenna with the same size of substrate to help and can enhance the antenna efficiency. On the front side of the patch antenna, a slight cut-out on the rectangular patch from bottom side has been considered, which can assist to enhance the bandwidth and alter the location of resonance frequency. Furthermore, the antenna design was constructed to work in different resonant

frequencies which are at 2.8 GHz, 3.9 GHz, 5GHz and 5.6GHz. All optimizations and modifications in the design (e.g., introducing cut-out, slot, ground, sizes, thickness) will enhance the efficiency of the antenna and emphasize return loss at specific resonance frequency and all these importance have been considered.

D. Phantom Brain Model

According to study [12] and its calculations, table1 shows the obtained material parameters (ϵ and σ) dielectric properties for the circular brain structure, which indicate that both the conductivity and permittivity for the different frequencies from 3 GHz to 8 GHz. The phantom brain model was designed using CST software.

Table 1: Dielectric Properties of Different Layers in Head Phantom

Tissue	Permittivity (ϵ)	Conductivity (σ)
Brain	43.22	1.29
CSF	70.1	2.3
Dura	46	0.9
Bone	5.6	0.03
Fat	5.54	0.04
Skin	45	0.73
Tumor	55	7

it can be seen from figure 2 that the phantom head involves of six layers as outer Skin, Fat, Bone (skull), Dura, CSF, and Brain. Figure 2 illustrates the brain model.

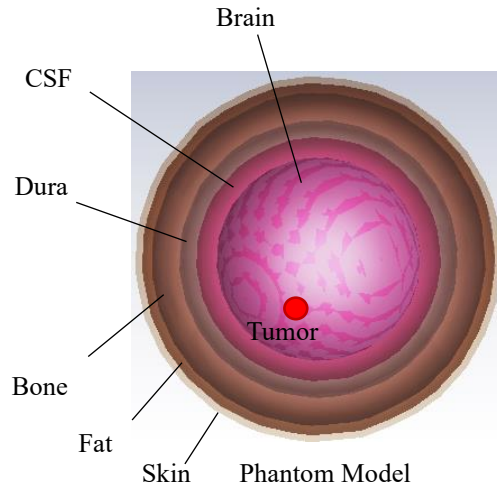


Figure 2. Phantom Head Model and Layers

III. RESULTS

A head-model is constructed by using the CST software to assess the entire system's act on detecting cancer cell which is using as a realistic phantom. All dielectric properties such as conductivity and permittivity were considered in different

layers. The position of the patch antenna was changing continually to collect the backscattering signals from different sides. In the result section a comparison study has been conducted and discussed for by using different resonance frequencies at 2.8 GHz, 3.9 GHz, 5GHz and 5.6GHz and with/without cancer cells as shown in figure 3.

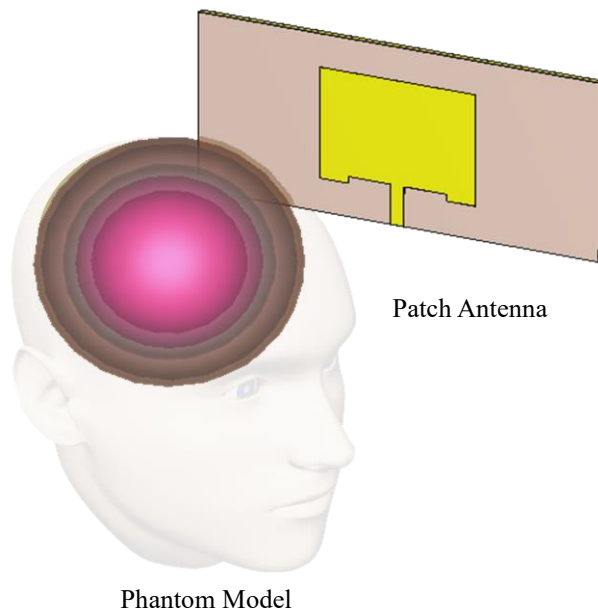


Figure 3. Antenna Patch Sensor with Phantom Brain Model

A Low-Cost Patch-Antenna for Non-Invasive Brain Cell Detection

A. Return Loss:

The first parameter that considered and analyzed is return loss (S11) at resonance frequency of 2.8 GHz, 3.9 GHz, 5GHz

and 5.6GHz. Each reflectance shows below -10 dB which complies with criteria. Figure 4 shows the graphs of return loss profile for reflector (S11) antenna sensor for both normal brain figure 4 (a) and affected cancerous brain figure 4 (b).

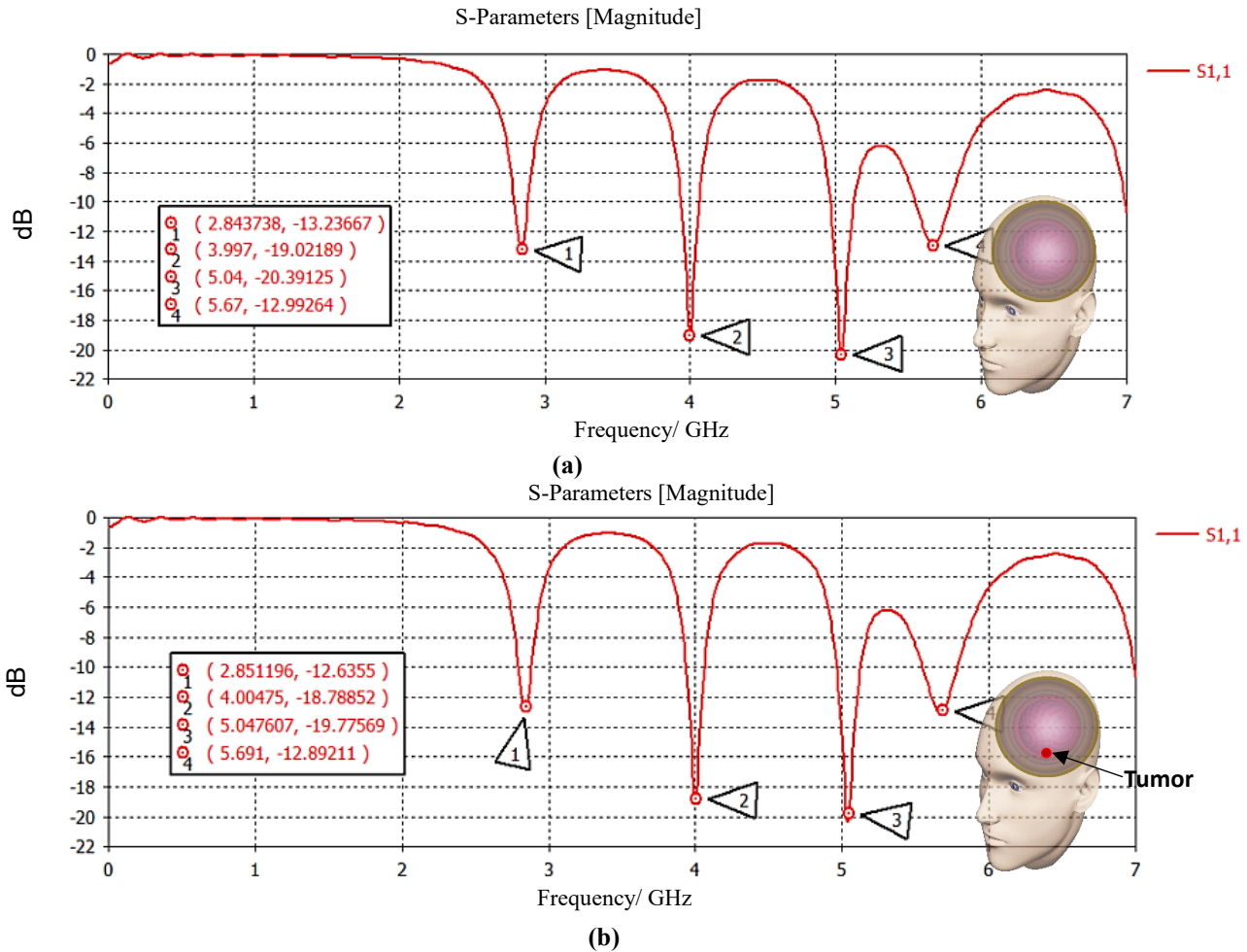


Figure 4. Return Loss Profile for Reflector (S11) Antenna Sensor, (A) without Tumor and (B) With Tumor Cell

It can be seen from figures 4 that at resonance frequency of 2.8 GHz, the phase shift between a normal and affected cell is around 7.45 MHz, whereas at the frequency of 3.9 GHz, the phase difference is around 7.75 MHz. At 5 GHz, the difference is 7.60 MHz and at the higher frequency of 5.6

GHz, the phase difference is around 21 GHz. Table 2 summarizes the depth value of return loss (S11) at each resonance frequency and corresponding phase difference/depth value without/with tumor cell.

Table 2: Resonance Frequencies and Difference Values Without/With Tumor Cell

Without Tumor Cell		With Tumor Cell		Phase Difference	Depth Value Difference
Frequency (GHz)	S11 (dB)	Frequency (GHz)	S11 (dB)	Frequency (MHz)	S11 (dB)
2.843738	-13.23667	2.851196	-12.6355	7.458	-0.60
3.997	-19.02189	4.00475	-18.7885	7.75	-0.23
5.04	-20.39125	5.047607	-19.7757	7.607	-0.62
5.67	-12.99264	5.691	-12.8921	21.0	-0.10

B. The Voltage Standing Wave Ratio (VSWR)

The VSWR is one of the parameters that is used in the design to indicate the mismatch between the feed line

connecting to the antenna patch. The minimum level in the allowable range (i.e.) below 2 can be obtained in our design. The results of the antenna design shown the value of VSWR at the resonance frequencies below Figure 5.

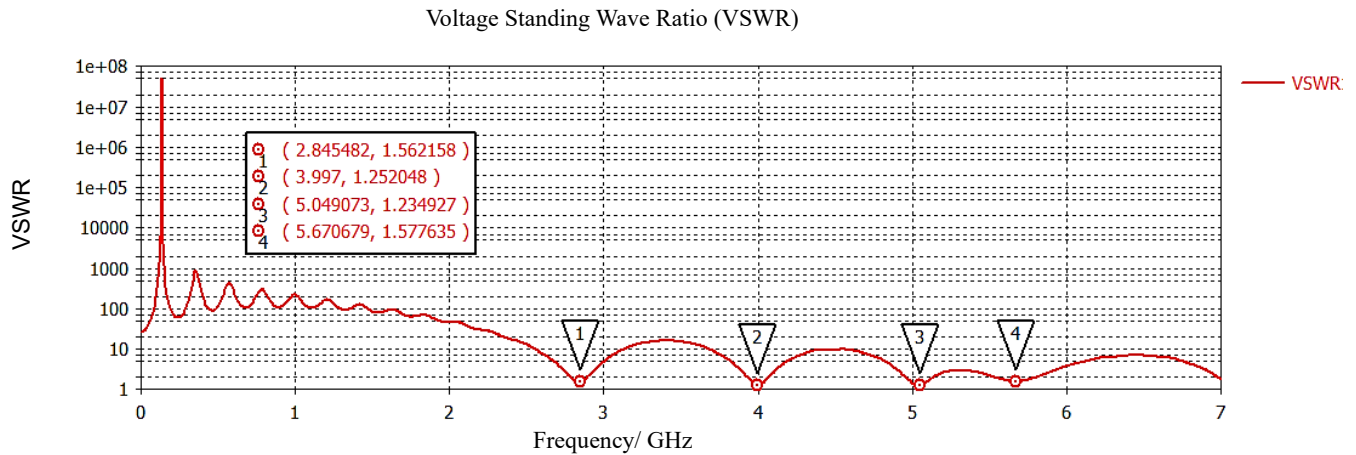
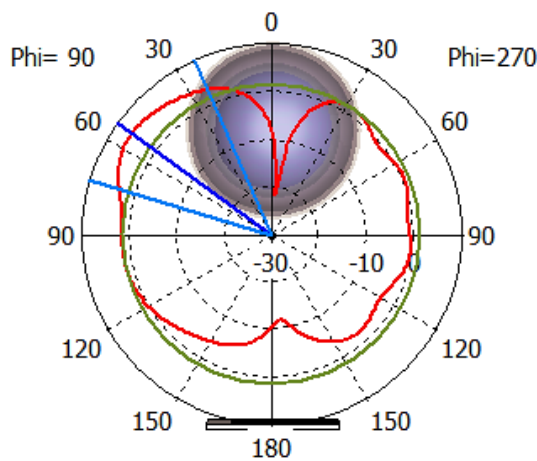


Figure 5. The Voltage Standing Wave Ratio (VSWR)

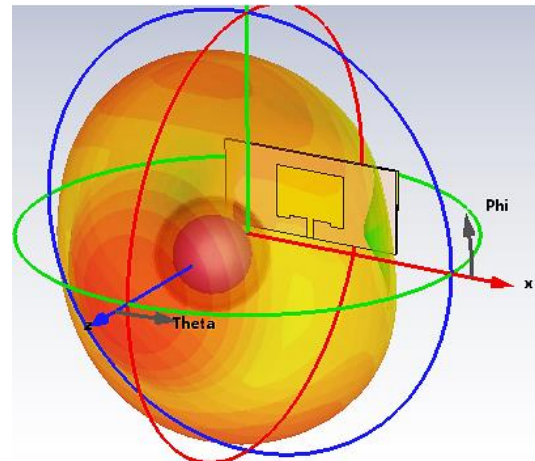
At the resonance frequencies 2.84, 3.99, 5.04 and 5.67 GHz, the VSWR values are 1.56, 1.25, 1.23 and 1.57 respectively. All VSWR values are under 2 which is suitable for the application. Thus, the antenna design is described as having a “Good Match” and when the value of VSWR overdoes 2 for a frequency of interest, it means that the design of the antenna is poorly matched. In our design, all values of VSWR are less than < 2 which indicate that the values in acceptable range and great match.

C. Radiation Pattern

The theta and phi components referred to a basic spherical coordinate system measurement. The spherical coordinates relate to the Cartesian axes: Theta = 0 for 360 and Phi = 0 for x-z Cut, Phi = 90 for y-z Cut. The x-z plane ($\phi = 0$) is referred to E-plane (x-z plane) whereas the y-z plane ($\phi = 90$) is referred to the H planes, respectively. The radiation pattern of proposed antenna in and H-plane (y-z plane) is shown in the figure 6 (a) and (b), and the 3-Dimensional radiation pattern is shown in Fig 6 (b). The beams in E-plane and H-plane are favorite because the primary lobes orientation is stable with broadside beams.



(a) 2-D radiation



(b) 3-D far-field

Figure 6. Radiation Pattern of the Patch Antenna in H-Plane (Y-Z Plane) and E-Plane (X-Z Plane)

From figure 6 (a), the main lobe magnitude = 6.22 dBi, the main lobe direction = 54.0 deg. and the angular width (3dB) = 49.3 deg. The simulated gain and directivity plotted and calculated for all resonance frequencies. The observed gain and directivity of each resonance frequency is summarized in table 3.

Table 3: Gain and Directivity at Resonance Frequencies

Frequency (GHz)	Gain (dBi)	Directivity (dBi)
2.84	2.72	7.34
5.04	0.30	6.61
5.68	3.75	8.12

D. Specific Absorption Rate (SAR)

One of the critical parameters is SAR absorption rate of radiation. To avoid health risk, the specific absorption rate (SAR) must not exceed 2 Watts per kilogram. The International Commission on Non-Ionizing Radiation Protection (ICNIRP) has recommended the limit of SAR Since 1998.

The SAR is obtained by dividing the total power absorbed in the human body by the full body weight. A local SAR is calculated and given as a numerical value per volume element and becomes a space distribution function. The Telecommunication Technology Council Agenda No. 89 and CENELEC 1995 is specified typical SAR values averaged in tissue masses of around 10g, whereas the value of 1g is adopted by ANSI/IEEE C95.1-1992 of the United States. A cuboid averaging volume is used. Thus, in this work a 10g and 1g of mass have been calculated and given the maximum SAR of 1.3 W/kg for 10g, and for 1g the maximum SAR is 2.1 W/kg.

IV. DISCUSSION

The antenna design was modeled and simulated by using CST-studio; the design was completed and contained layers of antenna with a full ground plane and patch with no slot. By using the full ground plane, the return loss was excellent and less than -10dB for all resonance frequencies. On the other hand, the SAR radiation was on boarder-line value of 2.1 W/kg at 1g maximum SAR. For the 10 grams of tissue, the maximum SAR of 1.3 W/kg which is in acceptable range less than < 1.6 w/kg. The SAR in simple terms refers to the rate at which the body absorbs RF energy. Thus, the antenna design in this work is suitable for biomedical applications.

Even though the phase difference at upper-band frequency of 5.67 GHz is 21 MHz, the depth value difference is worse at around -0.10 dB. The resolution of middle-band frequency of 3.99 and 5 GHz are significantly better in terms of return loss of -18.78 and -19.77 dB. However, the phase difference in the middle-band is less than that found in the upper-band by around 14 MHz. In addition, the depth value difference of return loss in the middle-band is notable and could be used as a reliable indicator of tumor cells present. At lower-band frequency of 2.84 GHz, the depth difference between both measurements (without/with tumor cell) is -0.60dB.

In addition, the resonance frequency was around 6 GHz and distant from lower band frequency which is not valuable for deep penetration. Then, the antenna was enhanced by introducing a cut around the two-edge bottom side of the patch antenna by 1.5 mm width and 6.5 mm length. The resonance frequency moves to lower band frequency around ~3 GHz, and we obtained the four resonance frequencies at 2.8 GHz, 3.9 GHz, 5GHz and 5.6GHz.

Accepted power and absorbed power: In both instances (without/with tumor), the stimulated power remained constant at 0.5 W. However, there were slight disparities in the accepted power: 0.476622 W for the non-tumor phantom and 0.47487 W for the tumor phantom. This suggests that the tumor's presence causes a slight modification in the way the tissue accepts power. In the tumor case, the absorbed power was marginally higher at 0.273287 W, as compared to the non-tumor case, which had an absorbed power of 0.271856 W. The total Specific Absorption Rate (SAR) in the tumor phantom was 0.42595 W/kg, which was lower than the SAR in the non-tumor phantom, which was 0.437733 W/kg. Indications point to the tumor impacting the dispersion of assimilated energy. Furthermore, the maximum specific absorption rate (SAR) was significantly lower in the tumor scenario in comparison to the non-tumor scenario. This

distinction is crucial as it emphasizes how the existence of a tumor can impact the specific points of absorption within the tissue. The highest specific absorption rate (SAR) measured over 10 grams of tissue was lower in the tumor scenario (1.39596 W/kg) compared to the non-tumor scenario (1.64121 W/kg). The maximum SAR point's coordinates experienced a slight shift, indicating a modification in the local energy absorption pattern because of the tumor's presence.

A higher penetration depth can be produced by a lower frequency with a lower resolution. Meanwhile, a better resolution can be generated by a higher frequency, but the penetration depth will be lesser as seen in the comparison study on table 2. Low frequencies band provide deeper penetration (lower loss), although higher frequencies band offer better resolution range in terms of phase shift but provides less depth value difference: hence, the choice of middle-band as an appropriate operating frequency ensuring internal views of normal/tumor brain with good depth penetration and high resolution. In brief, a higher band (upper band) frequency provides resolution but with less penetration and could miss the tumor cell if it is deeper. Thus, middle-band frequency is preferable as shown in the results. More than one antenna patch sensor can be mounted around the head to overcome the penetration issue and localization of the tumor cell. In the case of one patch antenna sensor is far away from the tumor, the other one could be closer and can detect it easily. The difference is attributed between return loss and its depth value as well as the frequency phase shift measurements due to the absence (normal cell) and presence of tumor cell. Moreover, the SAR analysis uncovers significant disparities in the way energy is absorbed and distributed between cases with tumors and cases without tumors. These results are acceptable and require further investigation into practical used.

V. CONCLUSION

A new patch antenna was designed for brain tumor detection at multiple resonance frequency of 2.8 GHz, 3.9 GHz, 5GHz and 5.6GHz. The CST Studie was used to model and simulate both antenna and phantom head. The realized of the antenna design at the resonance frequencies (return losses at the middle-band frequency) were -19dB while at higher or upper band frequency is around -12dB. It also observed from work that even though the higher band frequency is less than a middle band frequency in terms of return loss depth, but the higher band frequency provides identifiable detection and higher resolution (recognizable phase shift value) and better than the lower band frequency. A comparison study of antenna performance at different resonance frequencies was conducted. The phantom model was studied and evaluate with and without tumor cell and show the validation of the approach. Important parameters such as gain, directivity, VSWR, impedance matching and SAR were considered in the patch antenna design, and all values are recommended and meet the requirements and organizations standard.



The proposed design is a harmless device for biomedical applications of brain tumor detection.

ACKNOWLEDGMENTS

The author acknowledges and would like to thank the Ministry of Higher Education in the Kingdom of Saudi Arabia represented at Taif University, Taif, Saudi Arabia KSA.

DECLARATION STATEMENT

Funding	No, I did not receive.
Conflicts of Interest	No conflicts of interest to the best of our knowledge.
Ethical Approval and Consent to Participate	No, the article does not require ethical approval and consent to participate with evidence.
Availability of Data and Material/ Data Access Statement	Not relevant.
Authors Contributions	I am only the sole author of this article;

REFERENCES

- R. L. Siegel, K. D. Miller, and A. Jemal, "Cancer statistics, 2017," *CA: A Cancer Journal for Clinicians*, vol. 67, no. 1, pp. 7–30, 2017. <https://doi.org/10.3322/caac.21387>
- B. J. Mohammed, A. M. Abbosh, S. Mustafa, and D. Ireland, "Microwave system for head imaging," *IEEE Transactions on Instrumentation and Measurement*, vol. 63, no. 1, pp. 117–123, 2014. <https://doi.org/10.1109/TIM.2013.2277562>
- A. Hossain, M.T. Islam, M.E.H. Chowdhury, H. Rmili and M. A Samsuzzaman "Planar Ultrawideband Patch Antenna Array for Microwave Breast Tumor Detection". *Materials* 2020, 13, 4918. [PubMed]. <https://doi.org/10.3390/ma13214918>
- M.A.Aldhaeebi, K. Alzoubi, T.S. Almoneef, S.M. Bamatraf, , H. Attia and O.M. Ramahi "Review of Microwaves Techniques for Breast Cancer Detection". *Sensors* 2020, 20, 2390. <https://doi.org/10.3390/s20082390>
- M.Z. Mahmud, M.T Islam, N. Misran, S. Kibria, and M.Samsuzzaman, "Microwave Imaging for Breast Tumor Detection Using Uniplanar AMC Based CPW-Fed Microstrip Antenna". *IEEE Access* 2018, 6, 44763–44775. <https://doi.org/10.1109/ACCESS.2018.2859434>
- M. Ostadrahimi, P. Mojabi, S. Noghianian, L. Shafai, S. Pistorius, and J. Lovetri, "A novel microwave tomography system based on the scattering probe technique," *IEEE Transactions on Instrumentation and Measurement*, vol. 61, no. 2, pp. 379–390, 2012. <https://doi.org/10.1109/TIM.2011.2161931>
- F. S. G. B. Barnes, *Handbook of Biological Effects of Electromagnetic Fields*, CRC/Taylor & Francis, Boca Raton, FL, USA, 2007
- N. K. Nikolova, "Microwave imaging for breast cancer," *IEEE Microwave Magazine*, vol. 12, no. 7, pp. 78–94, 2011. <https://doi.org/10.1109/MMM.2011.942702>
- A. E. Souvorov, A. E. Bulyshev, S. Y. Semenov, R. H. Svenson, and G. P. Tatsis, "Two-dimensional computer analysis of a microwave fat antenna array for breast cancer tomography," *IEEE Transactions on Microwave Theory and Techniques*, vol. 48, no. 8, pp. 1413–1415, 2000. <https://doi.org/10.1109/22.859490>
- M. Rokunuzzaman, M. Samsuzzaman, and M. T. Islam, "Unidirectional Wideband 3-D Antenna for Human Head-Imaging Application," *IEEE Antennas and Wireless Propagation Letters*, vol. 16, pp. 169–172, 2017. <https://doi.org/10.1109/LAWP.2016.2565610>
- I. Singh and V. S. Tripathi, "Microstrip patch antenna and its applications: a survey," *International Journal of Computer Applications in Technology*, vol. 2, no. 5, pp. 1595–1599, 2011. <https://doi.org/10.14569/IJACSA.2011.020319>
- R. Inum, Md. Masud Rana, K. N. Shushama, and Md. A. Quader, "EBG Based Microstrip Patch Antenna for Brain Tumor Detection via Scattering Parameters in Microwave Imaging System," *International Journal of Biomedical Imaging*, Volume 2018, Article ID 8241438, 12 pages. <https://doi.org/10.1155/2018/8241438>
- M. Hussein, F. Awwad, D. Jithin, H. Hasasna, K. Athamneh and R. Iratni, "Breast cancer cells exhibits specific dielectric signature in vitro using the open-ended coaxial probe technique from 200 MHz to 13.6 GHz," *Sci. Rep.* 2019, 9, 4681. <https://doi.org/10.1038/s41598-019-41124-1>
- Balanis, Constantine A. *Antenna Theory: Analysis and Design*. 3rd ed. Hoboken, NJ: John Wiley, 2005

- Jogi, V. K., & Gupta, S. (2020). MEMS Based Diagnosis of Breast Cancer. In *International Journal of Innovative Technology and Exploring Engineering* (Vol. 9, Issue 4, pp. 2500–2503). <https://doi.org/10.35940/ijitee.d1728.029420.15>.
- Kaur, M., & Goyal, Dr. S. (2020). Microstrip Patch Antenna Design for Early Breast Cancer Detection. In *International Journal of Recent Technology and Engineering (IJRTE)* (Vol. 8, Issue 6, pp. 2698–2705). <https://doi.org/10.35940/ijrte.f8449.038620>
- Dollera, Elmer B. (2019). Water Desalination System using Parabolic Trough with Varying Glass Thickness. In *International Journal of Engineering and Advanced Technology* (Vol. 9, Issue 1, pp. 6–11). <https://doi.org/10.35940/ijeat.a1004.109119.16>.
- Sharma, S. (2023). Use of Vein Finder to Overcome Factor Affecting Peripheral Intravenous Cannulation, Venipuncture, IV Insertion, and Blood Draws. In *Indian Journal of Design Engineering* (Vol. 3, Issue 2, pp. 1–4). <https://doi.org/10.54105/ijde.a8026.083223.17>.
- Paliwal, S., & Kalyan, B. S. (2022). Driver's Activity Detection System using Human antenna. In *Indian Journal of Energy and Energy Resources* (Vol. 1, Issue 3, pp. 4–6). <https://doi.org/10.54105/ijeer.c1007.051322>

AUTHOR PROFILE



Abdullah Alzahrani, BSc, MSc, PhD is Assistance Professor at Taif University, Electrical and Electronic department. He also works for two years as Research Associate in Electronic Smart Sensor at Electrical Engineering, Cambridge Graphene Centre (CGC), The University of Cambridge, UK. Before joining the University, Alzahrani worked at different institutes (College of Technology (KSA) and Loughborough University (UK)) and he also worked at start-up companies (Cerebrum Matter LTD, UK) that specialized on EEG and Alzheimer. The main area that he works with and focuses on are integrated smart sensors, Micro-devices, Biomedical wearable physiological-sensors, environmental sensors, embedded system and electronic, communication design. Alzahrani is a member of SPIE, IEEE as well as a reviewer board member of *Advanced Research in Electrical, Electronics and Instrumentation Journal*. Alzahrani is a venture member at Haydn Green Institute for Innovation and Entrepreneurship, the University of Nottingham, UK. Intellectual property (IP) about Magneto-resistive has been filed to Cambridge Enterprise, the University of Cambridge, UK.

Disclaimer/Publisher's Note: The statements, opinions and data contained in all publications are solely those of the individual author(s) and contributor(s) and not of the Blue Eyes Intelligence Engineering and Sciences Publication (BEIESP)/ journal and/or the editor(s). The Blue Eyes Intelligence Engineering and Sciences Publication (BEIESP) and/or the editor(s) disclaim responsibility for any injury to people or property resulting from any ideas, methods, instructions or products referred to in the content.

